THE JOURNAL OF PHYSICAL CHEMISTRY A

Article

Solvent Modulation of Aromatic Substituent Effects in Molecular Balances Controlled by CH-# Interactions

Bright U Emenike, Ronald A. Spinelle, Ambar Rosario, David W. Shinn, and Barney Yoo

J. Phys. Chem. A, **Just Accepted Manuscript** • DOI: 10.1021/acs.jpca.7b09910 • Publication Date (Web): 15 Jan 2018

ACS Publications

The Journal of Physical Chemistry A is published by the American Chemical Society. 1155 Sixteenth Street N.W., Washington, DC 20036

Solvent Modulation of Aromatic Substituent Effects in Molecular Balances Controlled by CH-π Interactions

Bright U. Emenike,[1,] Ronald A. Spinelle,[1] Ambar Rosario,[1] David W. Shinn,[2] and Barney Yoo[3]*

[1]Department of Chemistry, State of University of New York, Old Westbury, NY 11568

[2]Department of Math and Science, U.S. Merchant Marine Academy, Kings Point, NY 11024

[3]Department of Chemistry, Hunter College, City University of New York, New York, NY 10065

Corresponding Author

*emenikeb@oldwestbury.edu

ABSTRACT

CH-π aromatic interactions are ubiquitous in nature and are capable of regulating important chemical and biochemical processes. Solvation and aromatic substituent effects are known to perturb the CH-π aromatic interactions. However, the nature by which the two factors influence one another is relatively unexplored. Here we demonstrate experimentally that there is a quantitative correlation between substituent effects in CH-π interactions and the hydrogen-bond acceptor constants of the solvating molecule. The CH-π interaction energies were measured by the conformational study of a series of aryl-substituted molecular balances in which the conformational preferences depended on the relative strengths of the methyl and aryl CH-π interactions in the *folded* and *unfolded* states, respectively. Due to the favorable methyl-aromatic interactions, the balances were found to exist predominantly in the folded state. The observed substituent effect in the conformational preferences of the balances was controlled by the explicit solvation/desolvation of the aryl proton. The interpretation of the conformational free energy as a function of substituents and solvation using Hunter's solvation model revealed that a linear

relationship exists between the sensitivity of aromatic substituent effects (*i.e.*, the rho values ρ derived from Hammett plots) and the hydrogen-bond acceptor propensity (β_s) of the solvent molecule: $\rho = 0.06\beta_s - 0.04$.

Introduction

Aromatic interactions—such as π-π stacking, CH-π, cation-π interactions—are among the most prevalent non-covalent interactions present in both synthetic and natural systems.[1-2] Although aromatic interactions are naturally weak, their collective strength is significant and plays decisive roles in chemical and enzymatic catalysis,[3-6] protein folding,[7-8] template-directed synthesis,[9] and materials science.[10] The strength of non-covalent interactions can be tuned by changing the properties of the local environment through solvent[11-17] and substituent modulations.[18-22] While numerous studies have examined substituent effects in aromatic interactions through linear free energy relationships, studies on the potential synergy—or the lack thereof—between solvation and the efficiency of aromatic substituent effects are rare. Considering the ubiquity of aromatic interactions, it is imperative to understand the environmental factors that influence the efficacy of aromatic substituent effects. Such an understanding would immensely expand our knowledge and application of aromatic interactions to the benefit of rational design of drugs, catalysts, and related functional materials.

There are two broad mechanisms for substituent effects in aromatic interactions. In π-π stacking for instance, Hunter and Sanders[23] (HS) proposed that aromatic substituent effect arises from the changes in the π electron density of the aromatic ring. Intuitively, electron-withdrawing substituents reduce the π electron density and electron-donating substituents increase the π electron density. Although the HS model is accepted pervasively, Wheeler and Houk[24-25] (WH)

proposed an alternative model in which aromatic substituent effects are described exclusively in terms of the *direct* (through-space) interactions between the substituents and the nearest vertex of the *other* aromatic ring. Both the HS and WH models are useful for predicting substituent effects in aromatic interactions.[26] To the best of our knowledge, aromatic substituent effects in non-covalent interactions have never been examined in the context that they might be influenced by solvation. This knowledge gap could have ramifications for the efficiency of aromatic interactions in environments where the local property is discontinuous—such as in the protein environment.

In quantifying the CH-π aromatic interactions between the edge of a phenyl ester and the face of substituted aromatic rings (using a series of molecular torsion balances), Wilcox and co-workers[27] observed no substituent effects in chloroform; and as a result, they concluded that edge-to-face aromatic interactions must originate from dispersion forces. Diederich and co-workers[28] performed the same experiment—only this time, a different torsion balance containing a 4-(trifluoromethyl)phenyl ester was used—and found a linear Hammett plot, suggesting that edge-to-face aromatic interactions have an electrostatic origin. Although one might argue that both electrostatic and dispersion are intrinsic features of the edge-to-face aromatic interaction,[29] the different results seem to suggest that the mechanism of aromatic substituent effects is not entirely an intrinsic property of the associated aromatic interactions, but rather one that changes with solvation. Therefore, understanding the physical origin for this behavior would be paramount in molecular recognition events. The specific goal of the present study is to explore whether aromatic substituent effects in CH-π interactions is affected by the properties of the solvating media.

Experimental Section

Measurement of interaction energies (ΔG) and error analysis. The folded/unfolded ratios were measured by proton NMR spectra at room temperature (~ 25°C). All spectra were recorded on a *Bruker Avance* operating at 400 MHz for the ^{1}H nucleus. All samples were recorded as 15 mM solution. Before integration all spectra were line-fitted to 100% Lorentz functions.

Error Analysis. Standard deviation of the equilibrium constant K determined by multiple measurements and integration of the line-fitted (100% Lorentz functions) ^{1}H NMRspectra.

Because error resulting from integration is typically smaller (~ 1%) than the error resulting from the experimental standard deviation (~ 5%) for concentrations above 10 mM, the standard error applies equally to all experiments.[30-31]

$$\delta (\ln K) = \delta K/K = 0.05$$

$$\delta(\Delta G) = RT[\delta (\ln K)] = 0.03 \text{ kcal/mol}$$

Preparation of pentacene.[32] Solid $NaBH_4$ (1.23 g, 32.4 mmol) was slowly added to a 100 mL round bottom flask containing a suspension of pentacene-6,13-dione (500 mg, 1.62 mmol) in THF (60 mL) at 0 °C. After $NaBH_4$ addition was complete, the reaction vessel was purged with nitrogen gas and 2 mL of water was added. The reaction mixture was heated to 50 to 60 °C until homogeneous. After 2 hours of heating, THF was evaporated and water was added, and the reaction mixture was filtered. The solids were washed with copious amounts of water. After drying, 420 mg of a white solid was obtained, which was used directly in the next step.

To the product of the first step, $SnCl_2$. $2H_2O$ (0.72 g, 3.2 mmol), DMF (8 mL) and 10 mL of conc. HCl was added over ~ 30 seconds with stirring at 0 °C (ice-water bath) in the dark. The

resulting blue reaction mixture was stirred briefly (~15 s) at 0 °C before an additional 10 mL of conc. HCl was added over ~30 seconds followed by the rapid addition of 50 mL water. The deep blue solids were filtered and washed with 25 mL amounts of water followed by 10 mL acetone. All washings were performed in air in the dark. The blue solid was dried under reduced pressure yielding 0.36 g of pentacene (79% yield, over two steps).

Synthesis of molecular balances.[11] Pentacene (1 mmol, 278 mg) and 1 mmol of the appropriate substituted *N*-arylimide were mixed in a reaction tube containing 5 mL toluene. The reaction tube was sealed under nitrogen atmosphere and was placed in an oil bath at 100°C. After ~ 5 h, the dark-blue reaction solution turned light yellow, indicating the complete consumption of the pentacene. The reaction tube was cooled to room temperature and the crystalline product was collected by filtration. Further purification of the balance was achieved, when necessary, by flash column chromatography using ethyl acetate-hexane mixtures.

Balances **1a** and **1c** have been previously reported,[11, 13] while balance **1b**, **1d**, and **1e** are new and full characterization are shown below:

1b: Yield = 78%. ^{1}H NMR (400 MHz, MeCN-d_3) δ = 0.41 (s, 2H, major), 2.10 (s, 1H, minor), 3.59 (s, 2H), 4.82 (d, 1H) 5.09 (s, 2H), 6.58 (d, 1H, J = 8.4 Hz, minor), 6.90 (m, 1H), 7.23-7.97 (m, 16H). ^{13}C NMR (101 MHz, DMSO-d_6) δ = 15.5, 17.6, 45.2, 45.7, 47.1, 47.2, 122.9, 123. 0, 123.9, 124.3, 126.3, 126.4, 126.8, 126.9, 127.6, 127.8, 128.3, 129.1, 129.2, 130.6, 130.8, 132.5, 132.6, 132.9, 135.0, 135.1, 135.6, 136.0, 137.3, 137.9, 138.0, 138.4, 175.8, 175.9. HRMS calcd for $C_{33}H_{22}ClNO_2$ $[M+H]^+$ 500.1412, found 500.1407

1d: Yield = 81%. ^{1}H NMR (400 MHz, DMSO-d_6) δ = 0.34 (s, 2H, major), 1.95 (s, 1H, minor), 2.12 (s, 1H, mior), 2.19 (s, 2H, major), 3.61 (s, 2H, major), 3.67 (s, 1H, minor), 4.66 (d, 1H, J =

8.0 Hz, minor), 5.13 (s, 2H), 6.36 (d, 1H, J = 8.0 Hz, minor), 6.38 (d, 1H, J = 8.0 Hz), 6.77 (s, 1H), 6.87 (d, 1H, J = 8.0 Hz, major), 6.99 (m, 1H), 7.50 (m, 4H), .7.90 – 8.05 (m, 8H). ^{13}C NMR (101 MHz, $CDCl_3$) δ = 15.5, 15.6, 20.9, 21.0, 45.3, 45.7, 47.1, 47.1, 122.9, 123.0, 124.0, 126.2, 126.3, 126.8, 127.3, 127.5, 127.5, 127.7, 127.8, 128.0, 131.4, 131.6, 132.6, 132.6, 133.0, 134.9, 135.5, 135.8, 136.1, 138.3, 138.7, 139.4, 176.2, 176.3. HRMS calcd for $C_{34}H_{25}NO_2$ $[M+H]^+$ 480.1958, found 480.1956

1e: Yield = 84%. ^{1}H NMR (400 MHz, $CDCl_3$) δ = 0.47 (s, 2H, major), 2.05 (s, 1H, minor), 3.58 (s, 2H, major), 3.66 (s, 1H), 3.69 (s, 2H), 4.90 (d, 1H, J = 8.8 Hz), 5.15 (s, 2H), 6.14 (d, 1H, J = 8.8 Hz, minor), 6.46 (s, 1H, major), 6.71 (m, 1H), 6.87 (d, 1H, J = 8.8 Hz), 7.51 (m, 4H), 7.77 (m, 8H). ^{13}C NMR (101 MHz, DMSO-d_6) δ = 15.6, 17.9, 45.2, 45.7, 47.0, 47.0, 55.2, 60.4, 111.9, 112.0, 115.9, 116.0, 122.8, 123.0, 123.1, 123.3, 123.9, 124.2, 126.2, 126.2, 127.6, 127.8, 128.0, 128.2, 128.7, 129.1, 132.5, 135.7, 136.1, 136.6, 137.3, 138.2, 138.6, 159.9, 159.9, 176.4. HRMS calcd for $C_{34}H_{25}NO_3$ $[M+H]^+$ 496.1907, found 496.1904

Results

The *N*-aryl imide balances (Scheme 1), similar to the designs emerging from Shimizu's lab,[33-35] have proven useful in quantifying weak non-covalent interactions in solution. The methyl group at one of the *ortho* positions (of the rotatable *N*-aryl ring) allows the competing folded and unfolded conformers to be in equilibrium with distinctive NMR signals. The ratio of these conformers, measured by proton NMR integration at room temperature, provides a means for estimating the position of the conformational equilibrium and for calculating the folding energy according to equation 1. Thus, the folding energy (ΔG) value is the difference in the free energies

of the folded and unfolded conformers, where a negative ΔG value indicates the folded conformer is more stable than the unfolded conformer.

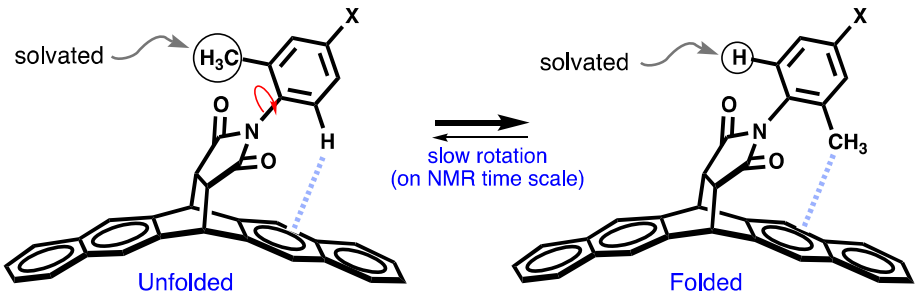

X = NO_2 (**1a**), Cl (**1b**), H (**1c**), CH_3 (**1d**), OCH_3 (**1e**)

Scheme 1. Derivatives of the *N*-aryl imide molecular balances used in this study.

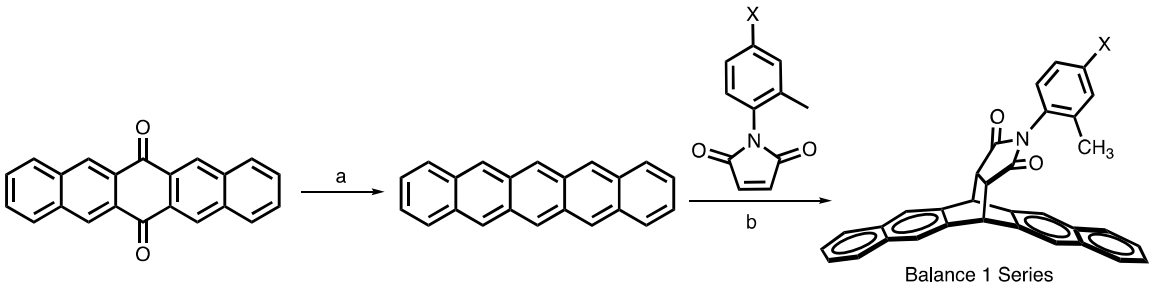

Scheme 2. Synthesis of balance **1**. **(**a) (i) $NaBH_4$/THF (ii) $SnCl_2.2H_2O$, HCl/DMF (b) Toluene, sealed-tube heat.

ΔG = -RTlnKeq = -RTln[folded]/[unfolded] (1)

The *N*-arylimide molecular balances are readily synthesized (as can be seen in scheme 2). Pentancene is prepared in a two-step reaction, which further undergoes a thermal Diels-Alder reaction with the appropriate substituted arylimide to produce the desired molecular torsion balances.

In the folded state, the *N*-aryl methyl is positioned directly above the π cloud of the naphthalene ring, which results in the formation of an intramolecular CH-π interaction while the aryl proton of the other *ortho* carbon is exposed to solvation. Consequently, the conformational preferences of the molecular balance are controlled by two factors: (1) the solvation/desolvation energies of the exchanging functional groups, and (2) the intrinsic energies of the aromatic interactions. Although aryl CH-π interaction is expected to be more energetic than methyl CH-π interaction,[36] the preference for the folded state can be attributed to a weak aryl CH-π interaction in the unfolded state, which is likely caused by the long distance between the aryl proton and the naphthalene carbon—3.56 Å at the B3LYP/6-31+G(d) level. To ascertain whether aromatic substituent effects are solvent dependent, various X substituents were placed on the *N*-aryl ring and the resulting changes in conformational free energy were determined as a function of solvation (Table 1). Positioning the X substituents on the *N*-aryl axis of rotation eliminates conformational bias arising from either (1) the differential *direct* interaction between the substituent and the aromatic ring,[24] (2) the differential position of the substituents,[37] or (3) the preferential solvation of the substituents.[38] The results (as summarized in Table 1) demonstrated that the folding energy varies as the substituents were changed, and, also, the folding energy of each X-substituted balance varies as a function of solvation. However, the degree of conformational free-energy change (ΔG) is apparently solvent dependent. For instance, ΔG spanned a range of 0.5 – 0.9 kcal/mol in DMSO, whereas the range was miniscule in chloroform, 0.26 – 0.29 kcal/mol.

Table 1. Measured folding Gibbs free energies of balances **1a - e** in different deuterated solvents.

Solvents[c]	X	(%)Folded[a]	ΔG (kcal/mol)[b]
DMSO	NO_2	82	-0.90
	Cl	76	-0.68
	H	70	-0.50
	CH_3	71	-0.53
	OCH_3	73	-0.59
THF	NO_2	76	-0.68
	Cl	71	-0.53
	H	67	-0.42
	CH_3	67	-0.42
	OCH_3	70	-0.50
Acetone	NO_2	73	-0.59
	Cl	70	-0.50
	H	65	-0.37
	CH_3	65	-0.37
	OCH_3	68	-0.45
Acetonitrile	NO_2	73	-0.59
	Cl	70	-0.50
	H	65	-0.37
	CH_3	65	-0.37
	OCH_3	67	-0.42
Benzene	NO_2	64	-0.34
	Cl	61	-0.26
	H	61	-0.26
	CH_3	60	-0.24
	OCH_3	62	-0.29
Chloroform	NO_2	61	-0.26
	Cl	62	-0.29
	H	61	-0.26
	CH_3	61	-0.26
	OCH_3	62	-0.29
CCl_4	NO_2	63	-0.31
	Cl	61	-0.26
	H	62	-0.29
	CH_3	ns	ns
	OCH_3	64	-0.34

[a] Determined by integration of ^{1}H NMR spectra at 298K. [b] Uncertainty ± 0.03 kcal/mol. [c] Deuderated solvents except for CCl_4. Ns = not soluble.

Discussion

The quantitative measurement of aromatic substituent effect is customarily assessed through the Hammett relationship, equation 2.[39] Here, the energies of aromatic substituent effects ($\Delta\Delta G_{ASE}$) were established more effectively with Hammett σ_m constants. The Hammett constant (σ_m) is the substituent constant for meta-substituents in benzene derivatives as defined by Hammett on the basis of the ionization of *meta*-substituted benzoic acids in water.[39] The slope of the Hammett plot (the rho value, ρ) describes the susceptibility of the balance's conformational preferences to the aromatic substituents.[40] The ρ parameter serves as the quantitative measure of aromatic substituent effects in the conformational preferences of the molecular balances. With standard reference to the substituent effects in the ionization of benzoic acids, a ρ value of 1 suggests a strong substituent effect while a zero ρ value is indicative of no substituent effect.

$$\Delta\Delta G_{ASE} = \Delta G_X - \Delta G_H = \rho\sigma_m \qquad (2)$$

The Hammett plots derived from the experimental results (Figure 1) indicated that aromatic substituent effects in the balance system varied with solvation because the slopes—although not as high as 1—varied with changing solvent properties. Specifically, the polar solvents (DMSO, THF, acetone, and acetonitrile) showed steeper slopes (0.29 – 0.50) than the non-polar solvents (benzene, CCl_4, and chloroform), which were close to zero (0 – 0.11). This trend seems to suggest that the slope diminishes as the polarity of the solvents is reduced. The lack of apparent substituent effects in the non-polar solvents could be attributed to the dominance of dispersion forces, which is one way of explaining poor Hammett correlations. [27] Conversely, we sought for a quantitative rationale based on Hunter's solvation model,[41] which has been useful in explaining

solvent effects in a variety of non-covalent interactions including hydrogen bond,[12] edge-to-face aromatic,[15, 42] CH-π,[11] and cation-π interactions.[13]

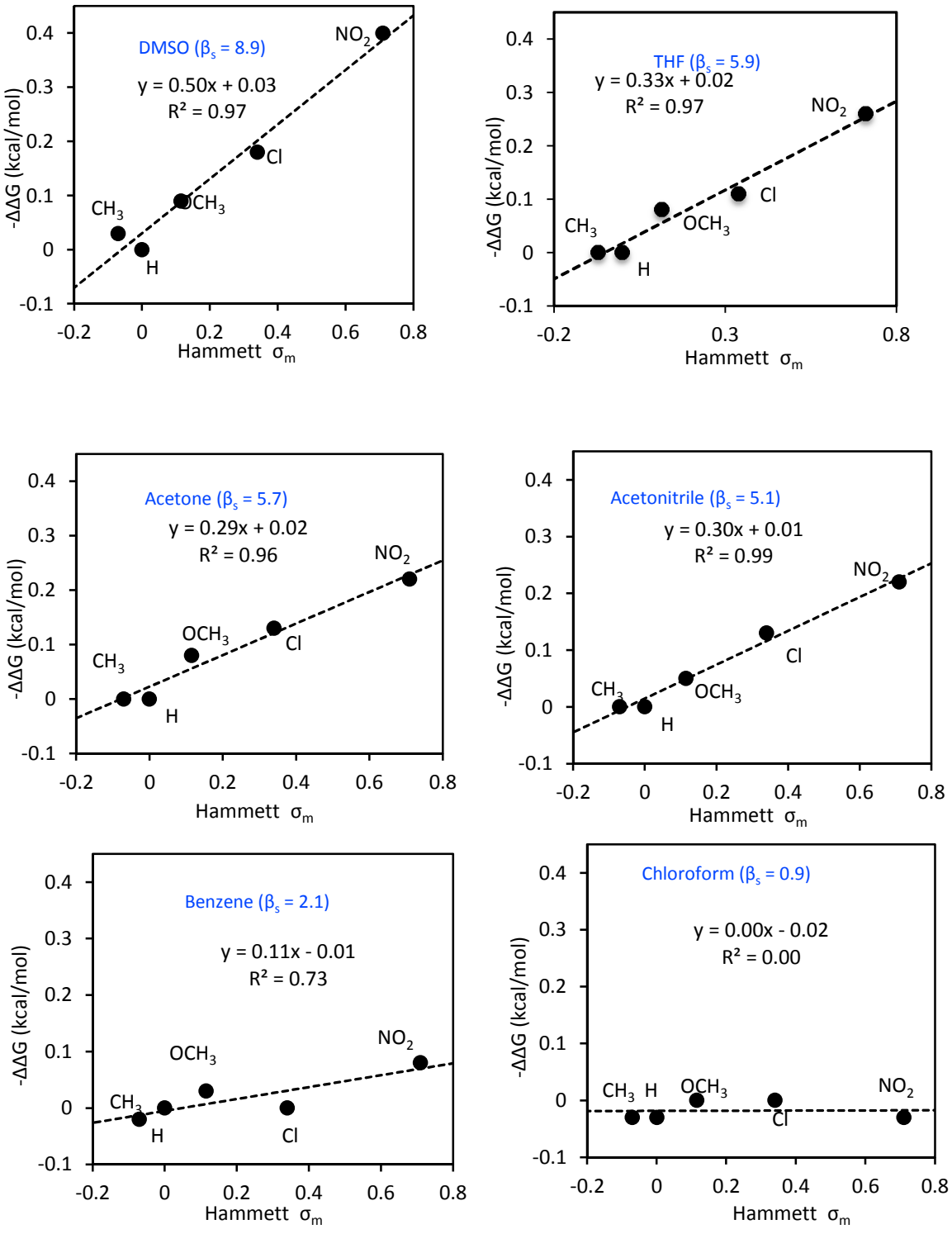

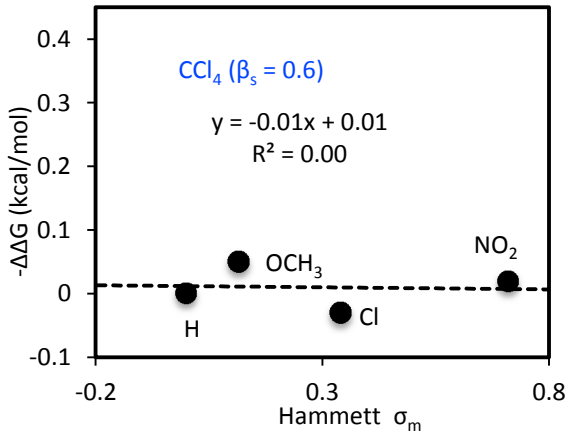

Figure 1. Correlation plot of $\Delta\Delta G_{ASE}$ and σ_m in various solvents.

Hunter's solvation model posits that solvation can be summarized as the collection of explicit electrostatic interactions ($\alpha\beta$) between solute and solvent molecules involving pairs of hydrogen bond donor (α) and acceptor (β).[41] This idea is analogous to the explicit solvation model put forth by Abraham and co-workers.[43-44] Even though all hydrogen-bond sites participate in this solvation model, only the sites indicated with blue circles in the schematic representation (Scheme 3) undergo changes between the folded and unfolded transition. The atoms that undergo solvation in one conformational state and desolvation in another state were discerned from the electrostatic map potential resulting from the structural optimization at the DFT B3LYP-D3/6-31+G(d) level. Thus, the conformational free energy change (ΔG) can be theorized in the form of equation 3, which considers: (1) the ΔG values for solvating the exposed hydrogen-bond sites in the folded ($\alpha_1\beta_s$ and $\alpha_2\beta_s$) and the unfolded states ($\alpha_s\beta$ and $\alpha_1\beta_s$) and (2) the intrinsic ΔG values for the intramolecular interactions ($\alpha_1\beta$ in the folded and $\alpha_2\beta$ in the unfolded states).

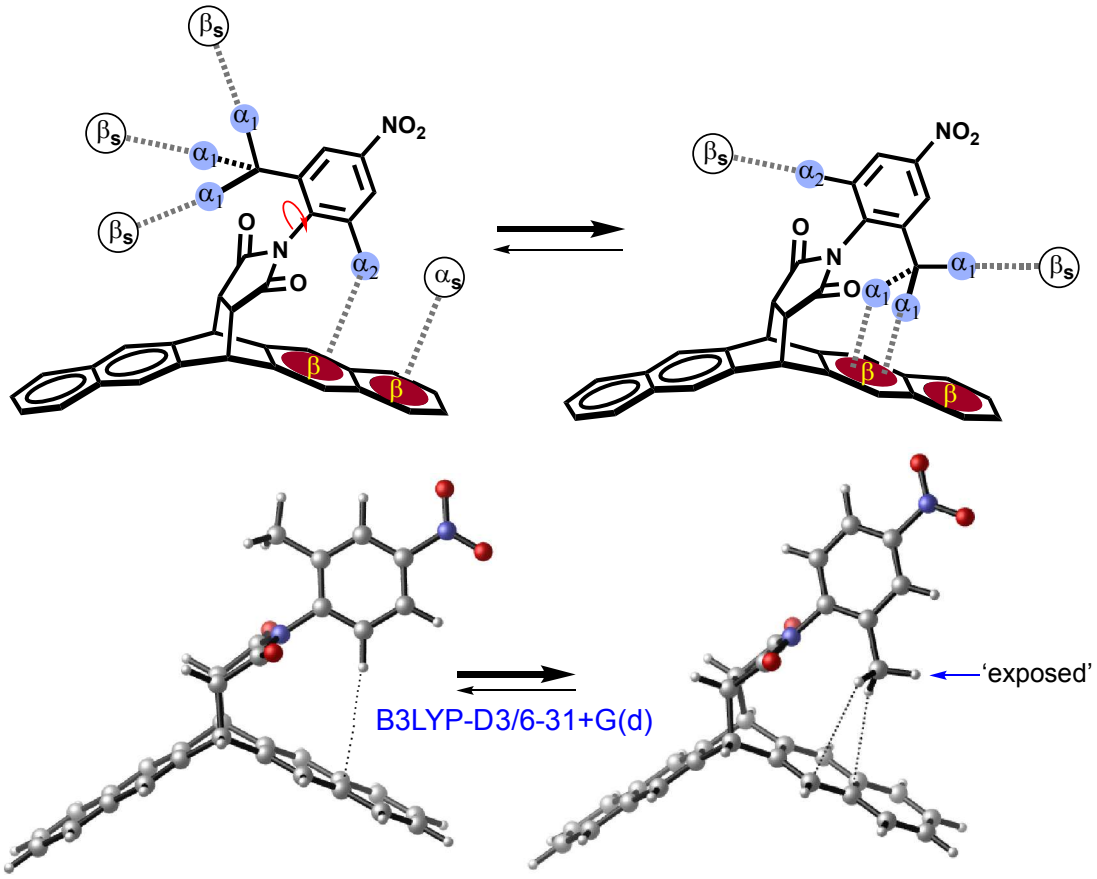

Scheme 3. Top: Schematic representation of explicit balance-solvent interactions in the folded and unfolded conformational states (top). Bottom: The DFT optimized folded-state conformation (at the B3LYP-D3/6-31+G(d) level) is in good agreement with the crystal structures of related molecular balances.[45]

$$\Delta G = (\alpha_s\beta + \alpha_2\beta + 3\alpha_1\beta_s) - (2\alpha_1\beta + \alpha_1\beta_s + \alpha_2\beta_s)$$

$$\Delta G = 2\alpha_1(\beta_s - \beta) - \alpha_2(\beta_s - \beta) + \alpha_s\beta \qquad (3)$$

Because inductive effects are characteristically distance dependent, it is reasonable to assume that the X substituent should affect only the acidities of α_1 and α_2 protons. In other words, the β value of the naphthalene π face—forming the CH-π interactions—should remain unperturbed by the variations of the X substituents. Thus, the energetics of the aromatic substituent effect

($\Delta\Delta G_{ASE}$), measured as $\Delta G_X - \Delta G_H$, can be expressed with equation 4, where change in the $\alpha_s\beta$ term (of equation 3) is zero.

$$\Delta\Delta G_{ASE} = \Delta G_X - \Delta G_H = (\Delta 2\alpha_1 - \Delta\alpha_2)(\beta_s - \beta) \quad (4)$$

Equation 4 is analogous to equation 2 because $\Delta\Delta G_{ASE}$ in both equations is directly proportional to solvent-dependent properties: ρ for equation 2 and $\beta_s - \beta$ for equation 4. In other words, there should be a linear relationship between the experimental ρ values and the solvent empirical β_s values if equation 4 is valid. Indeed, the plot of ρ as a function of β_s produced a nearly perfect linear correlation ($R^2 = 0.99$; Figure 2), which reflects on the *synergy that exists between aromatic substituent effects and solvation* in the molecular balance. Specifically, aromatic substituent effects in the balance system increased linearly with increasing propensity of the solvent to act as a hydrogen-bond acceptor: $\rho = 0.06\ \beta_s - 0.04$. This implies that the balance system will show little to no aromatic substituent effects ($\rho < 0.11$) in solvents of small β_s values ($\beta_s < 2.5$), which includes most non-polar solvents. An additional direct validation for equation 4 is that the $\Delta\Delta G_{ASE}$ term, for each substituent, correlates well with the solvents' β_s values (see supporting information).

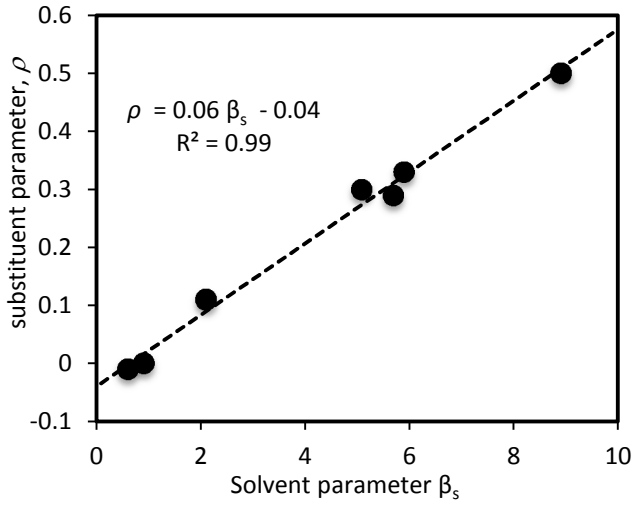

Figure 2. Correlation of rho values (ρ) as a function of solvents' hydrogen-bond acceptor constant (β_s). The β_s values were obtained from literature.[41]

Equation 4 provides the foundation for explaining the mechanism of the observed substituent effects in the molecular balance. Because aryl protons (such as Hα_2) are stronger hydrogen-bond donors than benzyl protons (such as Hα_1) *vide infra*,[17] it is reasonable to suggest that the folding of the balance is driven mainly by the favorable solvation of the exposed α_2 proton in the folded state. In order to substantiate this assertion, the values of α_1 and α_2 were estimated at the AM1 level following the protocols provided by Hunter.[41] When the substituent X = H, Hα_2 (0.9) is a stronger hydrogen-bond donor than Hα_1 (0.7). However, when X = NO_2, the difference in hydrogen-bond donor constants increased to 0.6 (*i.e.*, Hα_2 = 1.9 and Hα_1 = 1.3). This supports the idea that the increase in folding observed in solvents with strong hydrogen bond accepting propensities stem primarily from the preferential solvation of the Hα_2 proton. Conversely, the apparent lack of substituent effects in the non-polar solvents can be attributed to the small (near zero) values of the $\beta_s - \beta$ term. Because the hydrogen-bond acceptor constants of the non-polar solvents (β_s: benzene = 2.1 and chloroform = 0.9) closely matches that of the region of the

naphthalene π face (forming the aromatic interactions, β = 1.9), the two acceptor sites compete equally for the same donors; and this process is independent of the effective donor propensity of the interacting hydrogen.

If preferential solvation is responsible for the aromatic substituent effects observed in balance **1** series, improving the solvation of $H\alpha_2$ in the unfolded state—which is possible in a series of control models (**2a** – **2e**)—should lead to a reduced rho value. The control models possess aryl substituents equivalent to that of balance **1** series; however, balance **2** lacks the naphthalenyl ring present in balance **1**. The loss of the aromatic ring should increase the solvation of the $H\alpha_2$ proton in the unfolded state. While balance **1** showed the strongest substituent effects in DMSO ($\rho = 0.50$), the rho value observed for the control model, on the other hand, was much smaller ($\rho = 0.07$, Figure 3). This observation is consistent with the idea that the aromatic substituent effects are strongly influenced by the differential local solute-solvent interactions in the conformational states.

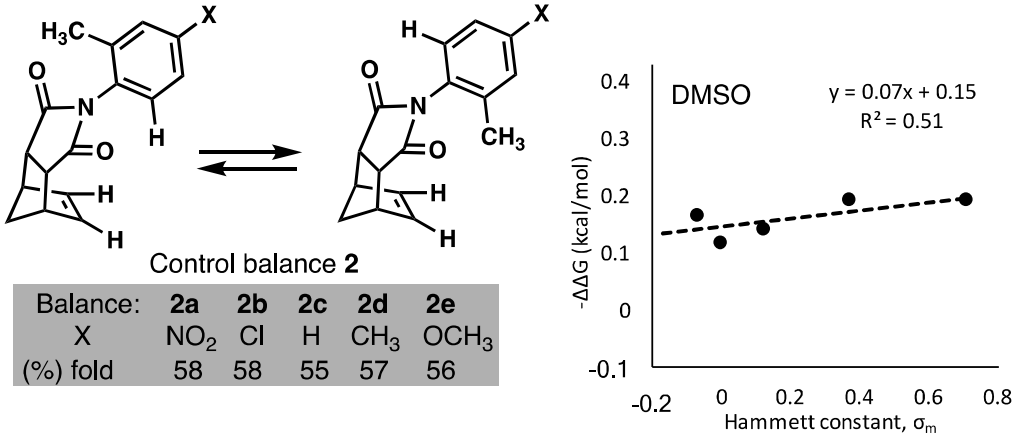

Figure 3. Conformational preferences of control balances (**2a** – **e**) as a function of Hammett constant measured in deuderated DMSO.

Conclusion

The goal of this study was to investigate whether or not aromatic substituent effects in CH-π interactions are solvent dependent and whether or not such a behavior can be explained quantitatively. These objectives were met by studying the conformational preferences of a series of substituted *N*-aryl molecular balances, which, with the aid of Hunter's solvation model,[41] revealed that aromatic substituent effects depend exclusively on solvents' hydrogen-bond acceptor propensity, β_s. In polar solvents (such as DMSO), the solvent molecule is a stronger hydrogen-bond acceptor than the π face of the naphthalene ring (*i.e.*, $\beta_s > \beta$); therefore, the aromatic substituent effect favors folding because of the preferential solvation of the *ortho* aryl proton. On the other hand, non-polar solvents (such as chloroform and benzene) have approximately similar β_s values as the π face of the naphthalene ring (*i.e.*, $\beta_s \approx \beta$); and as a result, it appears that the aromatic substituent effect have been washed out by solvation. Hammett plot is one of the tools for interpreting the mechanism of aromatic interactions, but the effects of solvation on such analyses are often ignored. As demonstrated in this work and related studies,[11, 13, 15, 42, 46] the delicate balance between desolvation and functional group interactions controls the behavior of closely related systems.

Supporting Information. Proton and carbon NMR spectra for balances **1** and **2** series. The following files are available free of charge.

Notes

The authors declare no competing financial interests.

ACKNOWLEDGMENT

We acknowledge donors of the American Chemical Society Petroleum Research Fund for support of this research (ACS-PRF # 55504-UNI4). DWS[47] and BUE thanks SUNY Old Westbury for Faculty Development Grants. AR acknowledges CSTEP (SUNY Old Westbury) for summer stipends.

REFERENCES

1. Burley, S. K.; Petsko, G. A. Aromatic-Aromatic Interaction - A Mechanism of Protein-Structure Stabilization. *Science* **1985,** *229*, 23-28.
2. Meyer, E. A.; Castellano, R. K.; Diederich, F. Interactions with Aromatic Rings in Chemical and Biological Recognition. *Angew. Chem. Int. Ed.* **2003,** *42*, 1210-1250.
3. Pecsi, I.; Leveles, I.; Harmat, V.; Vertessy, B. G.; Toth, J. Aromatic Stacking Between Nucleobase and Enzyme promotes Phosphate Ester Hydrolysis in dUTPase. *Nucleic Acids Res.* **2010,** *38*, 7179-7186.
4. Toth, G.; Watts, C. R.; Murphy, R. F.; Lovas, S. Significance of Aromatic-Backbone Amide Interactions in Protein Structure. *Proteins: Struct., Funct., And Genet.,* **2001,** *43*, 373-381.
5. Orlandi, M.; Coelho, J. A. S.; Hilton, M. J.; Toste, F. D.; Sigman, M. S. Parametrization of Non-covalent Interactions for Transition State Interrogation Applied to Asymmetric Catalysis. *J. Am. Chem. Soc.* **2017,** *139*, 6803-6806.
6. Seguin, T. J.; Wheeler, S. E. Stacking and Electrostatic Interactions Drive the Stereoselectivity of Silylium-Ion Asymmetric Counteranion-Directed Catalysis. *Angew. Chem. Int. Ed.* **2016,** *55*, 15889-15893.
7. Vacas, T.; Corzana, F.; Jimenez-Oses, G.; Gonzalez, C.; Gomez, A. M.; Bastida, A.; Revuelta, J.; Asensio, J. L. Role of Aromatic Rings in the Molecular Recognition of Aminoglycoside Antibiotics: Implications for Drug Design. *J. Am. Chem. Soc.* **2010,** *132*, 12074-12090.
8. McGaughey, G. B.; Gagne, M.; Rappe, A. K. Pi-stacking Interactions - Alive and well in Proteins. *J. Biol. Chem.* **1998,** *273*, 15458-15463.
9. Raymo, F. M.; Stoddart, J. F. Interlocked Macromolecules. *Chem. Rev.* **1999,** *99*, 1643-1663.
10. McNeil, A. J.; Muller, P.; Whitten, J. E.; Swager, T. M. Conjugated Polymers in an Arene Sandwich. *J. Am. Chem. Soc.* **2006,** *128*, 12426-12427.
11. Emenike, B. U.; Bey, S. N.; Bigelow, B. C.; Chakravartula, S. V. S. Quantitative Model for Rationalizing Solvent Effect in Noncovalent CH-Aryl interactions. *Chem. Sci.* **2016,** *7*, 1401-1407.
12. Cook, J. L.; Hunter, C. A.; Low, C. M. R.; Perez-Velasco, A.; Vinter, J. G. Solvent Effects on Hydrogen Bonding. *Angew. Chem. Int. Ed.* **2007,** *46*, 3706-3709.
13. Emenike, B. U.; Bey, S. N.; Spinelle, R. A.; Jones, J. T.; Yoo, B.; Zeller, M. Cationic CH-π Interactions as a Function of Solvation. *PCCP* **2016,** *18*, 30940-30945.

14. Yang, L.; Adam, C.; Cockroft, S. L. Quantifying Solvophobic Effects in Nonpolar Cohesive Interactions. *J. Am. Chem. Soc.* **2015,** *137*, 10084-10087.
15. Cockroft, S. L.; Hunter, C. A. Desolvation and Substituent Effects in Edge-to-Face Aromatic Interactions. *Chem. Commun.* **2009,** 3961-3963.
16. Adam, C.; Yang, L.; Cockroft, S. L. Partitioning Solvophobic and Dispersion Forces in Alkyl and Perfluoroalkyl Cohesion. *Angew. Chem. Int. Ed.* **2015,** *54*, 1164-1167.
17. Mati, I. K.; Adam, C.; Cockroft, S. L. Seeing Through Solvent Effects Using Molecular Balances. *Chem. Sci.* **2013,** *4*, 3965.
18. Cockroft, S. L.; Perkins, J.; Zonta, C.; Adams, H.; Spey, S. E.; Low, C. M. R.; Vinter, J. G.; Lawson, K. R.; Urch, C. J.; Hunter, C. A. Substituent Effects on Aromatic Stacking Interactions. *Org. Biomol. Chem.* **2007,** *5*, 1062-1080.
19. Carver, F. J.; Hunter, C. A.; Livingstone, D. J.; McCabe, J. F.; Seward, E. M. Substituent Effects on Edge-to-Face Aromatic Interactions. *Chem. Eur. J.* **2002,** *8*, 2848-2859.
20. Emenike, B. U.; Liu, A. T.; Naveo, E. P.; Roberts, J. D. Substituent Effects on Energetics of Peptide-Carboxylate Hydrogen Bonds as Studied by 1H NMR Spectroscopy: Implications for Enzyme Catalysis. *J. Org. Chem.* **2013,** *78*, 11765-11771.
21. Gung, B. W.; Emenike, B. U.; Lewis, M.; Kirschbaum, K. Quantification of CH-pi Interactions: Implications on How Substituent Effects Influence Aromatic Interactions. *Chem. Eur. J.* **2010,** *16*, 12357-12362.
22. Sinnokrot, M. O.; Sherrill, C. D. Substituent Effects in Pi-Pi Interactions: Sandwich and T-shaped Configurations. *J. Am. Chem. Soc.* **2004,** *126*, 7690-7697.
23. Hunter, C. A.; Sanders, J. K. M. The Nature of Pi-Pi Interactions. *J. Am. Chem. Soc.* **1990,** *112*, 5525-5534.
24. Wheeler, S. E.; Houk, K. N. Substituent Effects in the Benzene Dimer are Due to Direct Interactions of the Substituents with the Unsubstituted Benzene. *J. Am. Chem. Soc.* **2008,** *130*, 10854-10855.
25. Wheeler, S. E.; Houk, K. N. Substituent Effects in Cation/pi Interactions and Electrostatic Potentials above the Centers of Substituted Benzenes Are Due Primarily to Through-Space Effects of the Substituents. *J. Am. Chem. Soc.* **2009,** *131*, 3126-3127.
26. Ringer, A. L.; Sherrill, C. D. Substituent Effects in Sandwich Configurations of Multiply Substituted Benzene Dimers Are Not Solely Governed By Electrostatic Control. *J. Am. Chem. Soc.* **2009,** *131*, 4574-4575.
27. Kim, E.; Paliwal, S.; Wilcox, C. S. Measurements of Molecular Electrostatic Field Effects in Edge-to-Face Aromatic Interactions and CH-pi interactions with Implications for Protein Folding and Molecular Recognition. *J. Am. Chem. Soc.* **1998,** *120*, 11192-11193.
28. Fischer, F. R.; Schweizer, W. B.; Diederich, F. Substituent Effects on the Aromatic Edge-to-Face Interaction. *Chem. Commun.* **2008**, 4031-4022.
29. Wheeler, S. E.; Houk, K. N. Origin of Substituent Effects in Edge-to-Face Aryl-Aryl Interactions. *Mol. Phys.* **2009,** *107*, 749-760.
30. Gardarsson, H.; Schweizer, W. B.; Trapp, N.; Diederich, F. Structures and Properties of Molecular Torsion Balances to Decipher the Nature of Substituent Effects on the Aromatic Edge-to-Face Interaction. *Chem. Eur. J.* **2014,** *20*, 4608.
31. Ams, M. R.; Fields, M.; Grabnic, T.; Janesko, B. G.; Zeller, M.; Sheridan, R.; Shay, A. Unraveling the Role of Alkyl F on CH-pi Interactions and Uncovering the Tipping Point for Fluorophobicity. *J. Org. Chem.* **2015,** *80*, 7764-9.

32. Pramanik, C.; Miller, G. P. An Improved Synthesis of Pentacene: Rapid Access to a Benchmark Organic Semiconductor. *Molecules* **2012,** *17*, 4625-4633.
33. Carroll, W. R.; Pellechia, P.; Shimizu, K. D. A Rigid Molecular Balance for Measuring Face-to-Face Arene-Arene Interactions. *Org. Lett.* **2008,** *10*, 3547-3550.
34. Carroll, W. R.; Zhao, C.; Smith, M. D.; Pellechia, P. J.; Shimizu, K. D. A Molecular Balance for Measuring Aliphatic CH-pi Interactions. *Org. Lett.* **2011,** *13*, 4320-4323.
35. Zhao, C.; Parrish, R. M.; Smith, M. D.; Pellechia, P. J.; Sherrill, C. D.; Shimizu, K. D. Do Deuteriums Form Stronger CH−π Interactions? *J. Am. Chem. Soc.* **2012,** *134*, 14306-14309.
36. Alonso, M.; Woller, T.; Martín-Martínez, F. J.; Contreras-García, J.; Geerlings, P.; De Proft, F. Understanding the Fundamental Role of π/π, σ/σ, and σ/π Dispersion Interactions in Shaping Carbon-Based Materials. *Chem. Eur. J.* **2014,** *20*, 4931-4941.
37. Gung, B. W.; Emenike, B. U.; Alverez, C. N.; Rakovan, J.; Kirschbaum, K.; Jain, N. Relative Substituent Position on the Strength of Pi-Pi Stacking Interactions. *Tetrahedron Lett.* **2010,** *51*, 1648-1650.
38. Muchowska, K. B.; Adam, C.; Mati, I. K.; Cockroft, S. L. Electrostatic Modulation of Aromatic Rings via Explicit Solvation of Substituents. *J. Am. Chem. Soc.* **2013,** *135*, 9976-9979.
39. Hammett, L. P. The Effect of Structure Upon the Reactions of Organic Compounds. Benzene Derivatives. *J. Am. Chem. Soc.* **1937,** *59*, 96-103.
40. Hansch, C.; Leo, A.; Taft, R. W. A Survey of Hammett Substituent Constants and Resonance and Field Parameters. *Chem. Rev.* **1991,** *91*, 165-195.
41. Hunter, C. A. Quantifying Intermolecular Interactions: Guidelines for the Molecular Recognition Toolbox. *Angew. Chem. Int. Ed.* **2004,** *43*, 5310-5324.
42. Cockroft, S. L.; Hunter, C. A. Desolvation Tips the Balance: Solvent Effects on Aromatic Interactions. *Chem. Commun.* **2006**, 3806-3808.
43. Abraham, M. H. Scales of Solute Hydrogen-Bonding: Their Construction and Application to Physicochemical and Biochemical Processes. *Chem. Soc. Rev.* **1993,** *22*, 73-83.
44. Abraham, M. H.; Platts, J. A. Hydrogen Bond Structural Group Constants. *J. Org. Chem.* **2001,** *66*, 3484-3491.
45. Li, P.; Hwang, J.; Maier, J. M.; Zhao, C.; Kaborda, D. V.; Smith, M. D.; Pellechia, P. J.; Shimizu, K. D. Correlation Between Solid-State and Solution Conformational Ratios in a Series of N-(o-Tolyl)Succinimide Molecular Rotors. *Cryst. Growth Des.* **2015,** *15*, 3561-3564.
46. Maier, J. M.; Li, P.; Vik, E. C.; Yehl, C. J.; Strickland, S. M. S.; Shimizu, K. D. Measurement of Solvent OH−π Interactions Using a Molecular Balance. *J. Am. Chem. Soc.* **2017,** *139*, 6550-6553.
47. The authors declare that the views expressed in this article are the authors' own and not those of the U.S. Merchant Marine Academy, the Maritime Administration, the Department of Transportation or the United States government.

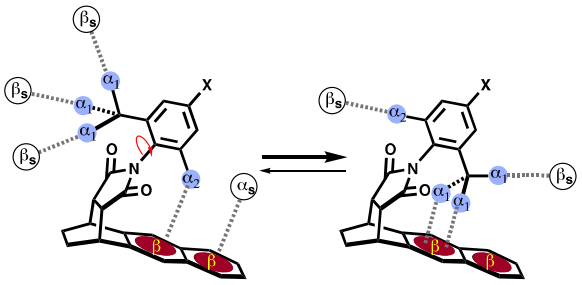

TOC Graphic